International Journal of Nanoscience
Vol. 10, Nos. 4 & 5 (2011) 681–685

DOI: 10.1142/S0219581X11008940

World Scientific
www.worldscientific.com

ZnO-NANOCRYSTALS IN STRONG CONFINEMENT REGIMES: INSIGHT ON RELAXATION DYNAMICS OF DEFECT STATES RESPONSIBLE FOR THE VISIBLE LUMINESCENCE

ARUNASISH LAYEK* and ARINDAM CHOWDHURY†
Department of Chemistry, Indian Institute of Technology Bombay
Powai, Mumbai 400076, India
**arunasish@chem.iitb.ac.in*
†*arindam@chem.iitb.ac.in*

The broad visible photoluminescence (PL) observed in ZnO nanocrystals (NCs) is widely attributed to multiple low lying surface-defects. We have performed steady state and time-resolved PL measurements on size-selected ZnO NCs in the strong confinement regimes. Our results show that radiative relaxation rates and coupling between excitons and surface defect states vary dramatically for sizes between 2 nm and 3 nm. Energy dependent PL lifetimes reveal that relaxation dynamics of these defect states in the blue- and red-edge of the emission are very different from each other.

Keywords: ZnO-nanocrystals; strong-confinement; defects; photoluminescence; relaxation dynamics.

1. Introduction

Among the naturally occurring wide band-gap materials, ZnO is technologically relevant because of its large band-gap (3.37 eV) and large exciton binging energy (60 meV) which render ZnO for variety of applications.[1] ZnO has a very small excitonic Bohr radius ($a_0 \sim 2.2$ nm) and shows quantum confinement below 7 nm,[2,3] the size regimes in which the band-gap and optical properties can be tuned by varying the size and shape of the nanocrystals (NCs).

Almost all reports concerning the optoelectronic properties of quantum-confined ZnO NCs synthesized using chemical routes, an intense and broad visible luminescence is observed. This luminescence centered around the green regions of the spectra has often been attributed to the recombination of charge-carriers in low energy defect states or radiative traps located at the surface of NCs.[4] The reason for such a broad and relatively intense emission band is still not fully understood, though it has been attributed to defects owing to unsaturated atoms or oxygen mediated peroxy linkages on the surface.[5]

Steady-state and time-resolved Photoluminescence (PL) spectroscopy of ZnO NCs have revealed the presence of multiple transitions underlying the emission envelope of the broad green emission. It has been shown that the blue-edge of the this broad emission band is due to the interaction of shallowly trapped holes with the free conduction band electrons, while the red-edge is due to the recombination of deeply trapped electrons with the free valence band holes.[6] Even though PL lifetime measurements on ZnO NCs revealed that these defect are indeed located on the surface, there are only a few reports on their emission energy dependence. Further, there are

no prior reports on the PL decay of defect states as a function of NC dimensions in the regimes of strong to intermediate confinement. We have performed steady state and time-resolved PL measurements on the defect emission of colloidal ZnO NCs between 2 and 4 nm diameters, and show how carrier recombination pathways vary when defect transitions are monitored.

2. Materials and Methods

2.1. *Synthesis of ZnO NCs*

Colloidal ZnO nanoparticles were synthesized following Ref. 1 with slight modifications. Briefly, 1.1 gm $Zn(OAc)_2 \cdot 2H_2O$ and 0.56 gm of KOH were dissolved in 50 mL of boiling ethanol in separate reaction vessels and allowed to cool to 0°C. The basic ethanolic solution was thoroughly mixed with zinc acetate solution maintained at 0°C. In order to obtain different sizes of ZnO NCs, colloidal solution was removed at regular intervals and poured into a 2 mM tertiary butyl phosphonic acid (TBPA) capping agent. The colloidal capped ZnO NCs was immediately cooled to −5°C to freeze the kinetics of further growth. Although capped NCs were found to be stable for days, all measurements were performed at 25°C, on freshly prepared samples.

2.2. *Steady-state and time resolved photoluminescence*

The capped colloidal ZnO NCs in ethanol were characterized by steady-state optical absorption with a UV-visible spectrophotometer (JASCO V570) and PL emission was performed with 300 nm excitation using a fluorescence spectrophotometer (Varian Cary Eclipse). Time-resolved PL decays were recorded on a time correlated single photon counting (TCSPC) system (IBH, UK) using a 340 nm excitation pulse (Nano LED 340) having an instrument response function of 800 ps. The PL decays were collected with an emission polarizer at the magic angle (54.7°).[7] The data was fitted using the iterative reconvolution method, to a sum of exponentials: $I(t) = \Sigma A_i \exp(-t/\tau_i)$, where ΣA_i is normalized to unity.

3. Results and Discussion

3.1. *Optical absorption measurements*

The optical absorption spectra of three different samples of colloidal ZnO NCs are shown in Fig. 1(a). The sharp onset of excitonic feature and the absence of a tail in its red-edge indicated a narrow size distribution. A reliable estimate of the band-gaps of quantum-confined NCs can be made from the excitonic absorption half maxima ($\lambda_{1/2}$) positions[1] which can then be used to obtain mean diameters (d) using Tight-Binding Model (TBM).[2] Using TBM, we have obtained d of synthesized NCs to be 2.2 ± 0.2, 3.3 ± 0.3, and 4.2 ± 0.4 nm. Two samples of ZnO NCs were independently checked by TEM measurements which were in good agreement (±0.5 nm) with the dimensions estimated by TBM.

3.2. *Steady-state PL measurements*

The PL emission spectra of ZnO NCs of three different sizes are shown in Fig. 1(a). Each spectrum

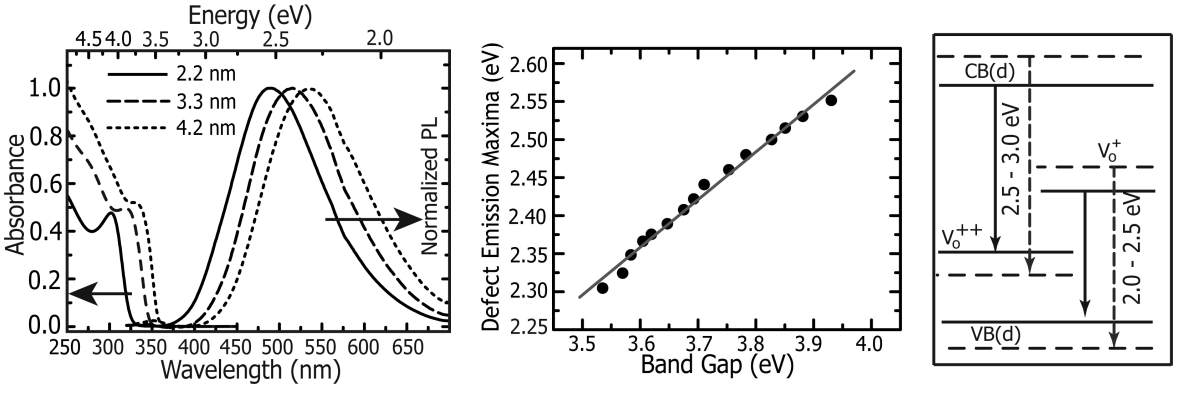

(a) (b) (c)

Fig. 1. (a) Electronic absorption and PL emission spectra of ZnO NCs of three different sizes, showing a red-shift of the λ_{max} with increasing size. (b) Defect λ_{em} plotted against the band-gap for NCs of decreasing size (4.4 → 2.1 nm). (c) Schematic of defect transitions from CB edge to V_o^{++} and V_o^{+} to the VB. The dotted lines indicate shifts in energies of the VB, CB and the defect levels.

consists of two emission bands: a very weak transition in the UV due to the excitonic recombination near band edge, and an intense broad band in the visible range (400−700 nm) involving defect related deep acceptor levels (V_o^{++}) and deep donor levels (V_o^{+}).[6] The defect emission envelope is composed of multiple transitions and it is likely that the blue-edge (2.5−3.0 eV) is due to recombination of free conduction band (CB) electrons with V_o^{++} of various energies, while several lower energy transitions result from recombination of deep trap electrons in V_o^{+} with free valence band (VB) holes.[8–11] Irrespective of the NC sizes between 2 nm and 4 nm, the shape of the emission envelope remains unchanged, while the PL emission maxima ($\lambda_{PL}^{\max}$) shifts continuously. A linear correlation is evident when the defect $\lambda_{PL}^{\max}$ is plotted against the NC band-gap (Fig. 1(b)). A similar behavior is observed if the defect $\lambda_{PL}^{\max}$ is plotted against the UV emission maxima. This clearly suggests that energies of V_o^{+} and V_o^{++}, shift alongside the CB and VB, respectively, with decreasing NC size. A schematic depicting the energy levels responsible for the defect transitions is shown in Fig. 1(c), where dotted lines indicate the shift of bands with decreasing particle size. It is very likely that there is an analogous energetic shift of the defect states in the sub-band levels due to strong quantum confinement.

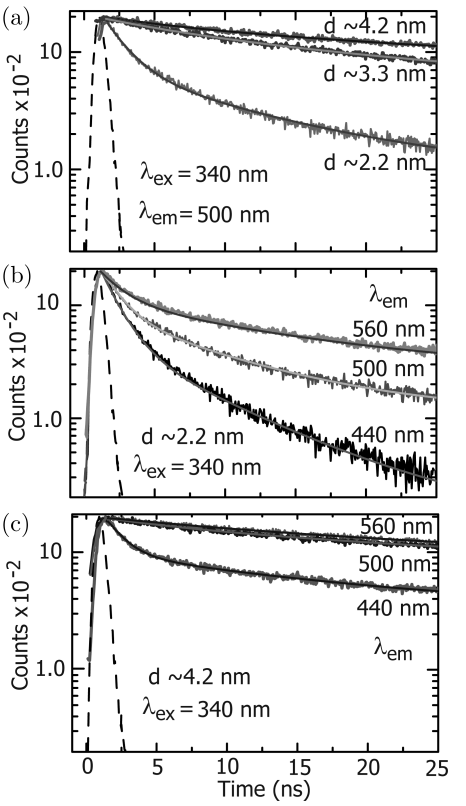

Fig. 2. (a) Visible PL decay curves obtained at 500 nm for ZnO NCs of diameters 2.2 nm, 3.3 nm, and 4.2 nm. Emission energy dependent decay traces for 2.2 nm (b) and 4.2 nm (c) ZnO NCs recorded at 440 nm, 500 nm, and 560 nm. The biexponential fit (solid lines) to the decay up to 25 ns is shown for clarity.

3.3. *Size dependence of radiative lifetimes*

Figure 2(a) shows the time-resolved PL data ($\lambda_{\max}^{PL} = 500$ nm) obtained for ZnO NCs of different dimensions in the strong and intermediate confinement regimes. The traces for all the three samples were incomplete and needed hundreds of nanoseconds for complete decay, suggesting deep-trap nature of some of the defect states. Nevertheless, decay profiles monitored up to 50 ns were typically bi-exponential for all the three sizes. Therefore, we focus here on the initial decay up to 50 ns which clearly has two well separated time-constants (τ_1 and τ_2). The decay parameters obtained from the fits to the biexponential is shown in Table 1.

In NC sizes between 2.2 nm and 4.2 nm diameters, radiative lifetimes vary significantly as a function of size. Qualitatively, the decay was found to be slower for larger NCs. Interestingly, NCs of diameters 2.2 nm showed a considerably faster decay as compared to both 3.2 nm and 4.2 nm samples. It is also evident that for increasing size beyond 3.3 nm, the decays change only slightly even though a correct trend is preserved. There was 4−6 fold increase in both the radiative lifetimes τ_1 and τ_2 with increase in particle size from 2.2 nm to 3.3 nm, while beyond 3.3 nm, τ_1 essentially remains unchanged and τ_2 increases slightly.

It is likely that surface defect states are responsible for the longer lifetimes for both τ_1 and τ_2 in the visible emission in ZnO NCs. It is evident that as the NC size becomes larger than the Bohr radius (∼2.4 nm), the coupling between the exciton and surface-states should reduce dramatically resulting in a longer lifetimes of these defect states. Since the relaxation rates are much faster for 2.2 nm NCs but are comparable for both 3.3 nm and 4.2 nm diameter NCs, it can be concluded that the electronic coupling between the excitons and the surface states is indeed very strong for NC diameters of ∼2.2 nm and reduces drastically with increasing size, up to ∼3 nm. Beyond this size range, the coupling becomes quite weak and shows a gradual reduction up to bulk levels. This data is very consistent with

Table 1. Time-resolved PL decay parameters using biexponential fits for size-selected ZnO NCs.

ZnO	$d \sim 2.2$ nm; $\lambda_{(PL)}^{Max} \sim 490$ nm					$d \sim 4.2$ nm; $\lambda_{(PL)}^{Max} \sim 535$ nm				
λ_{em} (nm)	τ_1 (ns)	A_1	τ_2 (ns)	A_2	χ^2	τ_1 (ns)	A_1	τ_2 (ns)	A_2	χ^2
440	1.36	0.97	7.04	0.03	1.06	1.75	0.82	25.9	0.18	1.10
500	1.67	0.87	10.2	0.13	1.10	6.30	0.28	38.1	0.72	1.04
560	2.16	0.82	17.7	0.18	1.12	9.70	0.21	41.9	0.79	1.02

band-gap changes in the strong confinement regime for ZnO, where band-gap varies dramatically with slight variation in NC diameter.[2]

3.4. *Emission energy dependence of radiative lifetimes*

Figures 2(b) and 2(c) shows the defect energy dependent carrier recombination dynamics for size-selected ZnO NCs at the blue-/red-edge as well as near the maxima of the visible emission spectra. Both the 2.2 nm and 4.2 nm NCs show pronounced wavelength dependence on the decay profiles. The PL decay was found to be much slower at lower energies (i.e., between 500 nm and 560 nm) irrespective of NC dimensions. This is likely because of involvement of multiple lower energy surface states where excitons eventually get trapped before getting deactivated via radiative or non-radiative pathways.[12] Nevertheless, the energy dependence of the decay is more pronounced for the NCs of 2.2 nm diameters (Fig. 2(b)) even though the fast component (τ_1) shows only small variation at different wavelengths (Table 1). For the 4.2 nm NCs however, there is a considerable increase in τ_1 when the emission is monitored at lower energies.

At the red-edge of the emission spectra (560 nm), radiative lifetimes are long for both the components τ_1 and τ_2. The decay profiles at 500 nm and above shows a clear saturation behavior ($\tau_2 \sim 40$ ns) for the larger NCs (Fig. 2(c)). This strongly suggests that the excitonic relaxation in the defect states between 2.5−3.0 eV are much faster compared to those at lower energies (2.0−2.5 eV), especially for NCs larger than 3 nm diameters.

The energy-dependent radiative lifetimes can be attributed to strong Coulomb interaction between the electron-hole pair in the form of total energy of the emitted photon: $E_{h\nu} = E_x - (D_+ - D_-) + e^2/\varepsilon R$, where D_+ and D_- are trap depths for the electron and hole separated by a distance R and measured with respect to the lowest delocalized state, E_x of the ZnO NCs. Close pairs with small R decay faster at higher energies while distant pairs do so at lower energies. Therefore, the distribution of such excited states at various trap sites is responsible for emissions with different lifetimes.[13,14]

4. Conclusion

We show that the energies of defect states in ZnO NCs responsible for visible emission shifts systematically alongside VB or CB even in the strong-confinement regime. Carrier relaxation processes in these defect states show severe size dependence in this regime which implies a dramatic reduction in the coupling between the excitons and the surface states beyond ∼2.5 nm diameters. Energy-dependent PL decays reveal that relaxation pathways through deep-donors (V_o^+) are much slower compared to transitions through deep acceptor levels (V_o^{++}).

Acknowledgment

We thank Professors S. Dhar, B. P. Singh, T. Kundu and A. Datta for valuable discussions and S. Banerjee for help with TCSPC data analyses. We thank the Department of Chemistry and IIT-Bombay for usage of Central Facility instruments and PhD scholarship to AL.

References

1. E. A. Meulenkamp, *J. Phys. Chem. B* **102**, 5566 (1998) and references therein.
2. R. Viswanatha, S. Sapra, B. Satpati, P. V. Satyam, B. N. Dev and D. D. Sarma, *J. Mater. Chem.* **14**, 661 (2004).
3. R. Viswanatha and D. D. Sarma, *Chem. Eur. J.* **12**, 180 (2006).
4. G. H. Schoenmakers, D. Vanmaekelbergh and J. J. Kelly, *J. Phys. Chem.* **100**, 3215 (1996).

5. R. C. Lima, L. R. Macario, J. W. M. Espinosa, V. M. Longo, R. Erlo, N. L. Marana, J. R. Sambrano, M. L. dos Santos, A. P. Moura, P. S. Pizani, J. Andre's, E. Longo and J. A. Varela, *J. Phys. Chem. A* **112**, 8970 (2008) and references therein.
6. L. Irimpan, V. P. N. Nampoori, P. Radhakrishnan, A. Deepthy and B. Krishnan, *J. Appl. Phys.* **102**, 063524 (2007).
7. S. Patel and A. Datta, *J. Phys. Chem. B* **111**, 10557 (2007).
8. L. E. Brus, *J. Chem. Phys.* **79**, 5566 (1983).
9. K. Vanheusden, C. H. Seager, W. L. Warren, D. R. Tallant and J. A. Voigt, *Appl. Phys. Lett.* **68**, 403 (1996).
10. S. Rakshit and S. Vasudevan, *J. Phys. Chem. C* **112**, 4531 (2008).
11. A. van Dijken, E. A. Meulenkamp, D. Vanmaekelbergh and A. Meijerink, *J. Lumin.* **90**, 123 (2000).
12. A. van Dijken, E. A. Meulenkamp, D. Vanmaekelbergh and A. Meijerink, *J. Lumin.* **87–89**, 454 (2000).
13. N. Chestnoy, T. D. Harris, R. Hull and L. E. Brus, *J. Phys. Chem.* **90**, 3393 (1986).
14. P. V. Kamat and B. Patrick, *J. Phys. Chem.* **96**, 6829 (1992).